

MEASUREMENTS OF THE GSI TRANSFER BEAM LINES ION OPTICS

M. Sapinski*, O. Geithner, S. Reimann, P. Schuett, M. Vossberg, B. Walasek-Hoehne,
GSI, Darmstadt, Germany
C. Hessler, CERN, Geneva, Switzerland

Abstract

GSI High Energy Beam Transfer lines (HEST) link the SIS18 synchrotron with two storage rings (Experimental Storage Ring and Cryring) and six experimental caves. The recent upgrades to HEST beam instrumentation enables precise measurements of beam properties along the lines and allow for faster and more precise beams setup on targets. Preliminary results of some of the measurements performed during runs in 2018 and 2019 are presented here. The focus is on response matrix measurements and quadrupole scans performed on HADES beam line. The errors and future improvements are discussed.

INTRODUCTION

The High Energy Beam Transfer lines (HEST, from German: Hochenergie-Strahlführung) in GSI Helmholtzzentrum (Darmstadt, Germany) is a system of almost 500 meters of beam lines linking SIS18 synchrotron with experimental caves and storage rings. In this paper we focus on a beam line leading to HADES experiment [1], with length of about 160 meters, described in [2].

Most of the beam line is straight however the angle between the axis of the HADES experiment and the axis of the beam extracted from SIS18 is 15° in horizontal plane. In vertical plane the axis is parallel to the beam axis, but about 70 cm above it. In order to direct the beam to the experiment, two 7.5° dipoles, at 128 and 143 meters from the synchrotron extraction point, tilted by $\pm 21.6^\circ$ with respect to the beam axis, are installed. We describe a series of measurements performed during the engineering run in 2018 and physics run in 2019.

TRAJECTORY RESPONSE MATRIX

The trajectory response matrix (TRM) measurement is done by registering the change of the beam position in response to a „kick” from the steering magnets. It is a good method to assess the quality of the beam line optics model independently of the twiss parameters at the beginning of the line. Results of the measurements are usually presented in a form of a matrix, where one dimension designates the steerer magnets and the other one, the beam position measuring devices like scintillating screens or multi-wire proportional chambers (MWPC). The elements of the matrix describe change of beam position in response to a „kick”. In addition to model verification, the TRM allows for a global correction of the beam trajectory.

The TRM measurement has been performed on November 27th, 2018, with $^{40}\text{Ar}^{18+}$ beam at 300 MeV/u and on April

1st, 2019 with $^{107}\text{Ag}^{45+}$ at 1230 MeV/u. In both measurements, the beam was extracted from SIS18 using 3rd order quadrupolar resonant extraction. Beam position was measured using four MWPCs with 0.5 mm spacing between the wires. The profiles are taken at a fixed time within the spill and the location of the beam center is usually calculated as a mean position of the registered distribution (Fig. 1).

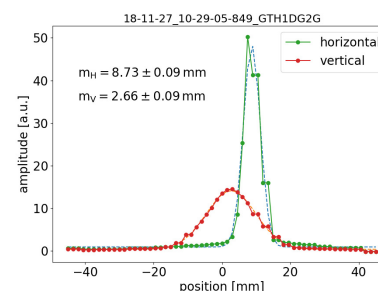


Figure 1: Example of a beam profiles measured with MWPC.

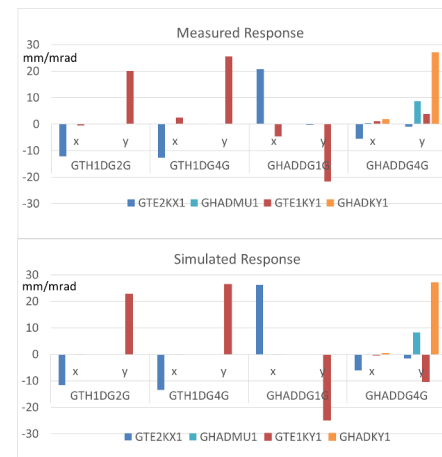


Figure 2: Measurement (upper) and modelling (bottom) of TRM.

The results of TRM measurement are illustrated in Fig. 2. In general, a good agreement between model and measurement is observed. The vertical response to a kick of the dipole GHADMU1 is much larger than the horizontal one. Differences between model and measurement are largest on the last grid. This is expected due to missing alignment data of the last elements. Future improvements of the model, and more precise TRM measurements in this area, using additional monitors, are planned.

* m.sapinski@gsi.de

BEAM POSITION DURING THE SPILL

Scintillating screens measure beam profile more precisely than MWPC. They are made of a moveable screen (chromox in our case), and a camera which registers the image of the beam-provoked scintillation. The system of scintillating screens installed in HEST is being upgraded from analog cameras, giving only an image of the beam spot on CRT screens, to a fully digital CUPID system [3]. Waiting for a full transition some of the cameras were digitized using frame grabbers [4] and it became possible to analyse the transverse beam profiles.

In November 2018, the camera located in the diagnose box GTH2DFA, was digitized. It was not possible to connect the trigger, therefore the frame grabber was in video-registration mode with rate of 25 frames per second. The video file is compressed using mpeg-2 format. This compression is lossy, what affects data quality as shown in Fig. 3. The profiles are fitted with Gaussian using python scipy module [5]. The errors on sigmas are small and χ^2 of the fits are good. The vertical profile is affected by fluctuations probably due to noise interfering with interlaced analog video signal transmission. The decay time of chromox scintillator is about 100 ms, therefore the afterglow affects the measurement.

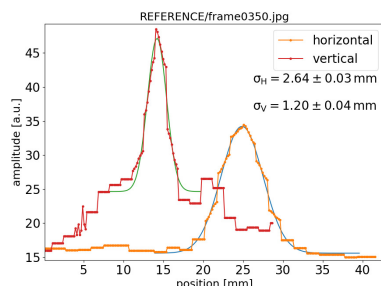


Figure 3: Example of beam profiles obtained with analog camera and a frame grabber on GTH2DFA screen.

The first series of measurements have been performed on December 14th, 2018, using $^{107}\text{Ag}^{45+}$ beam at 1580 MeV/u. During the spill the amplitude of the extraction bump at electrostatic septum was adjusted dynamically. Figure 4 shows the beam position evolution during the spill. As expected, the beam is very stable in vertical plane, however in horizontal plane it moves by almost 7 mm. The reason of the movement is the dispersion present at the screen and a change of the angle at the septum during the spill [6]. In the future the influence of these two effects will be distinguished by registering the $\Delta p/p$ of the circulating beam during the extraction, by measuring beam dispersion in the location of the screen and by measuring the change of the beam angle close to the extraction region.

QUADRUPOLE SCAN

Quadrupole scan allows to determine beam emittance and twiss parameters at the entrance of the quadrupole magnet. The scan is done by measuring the beam size on a down-

MOPGW024

132

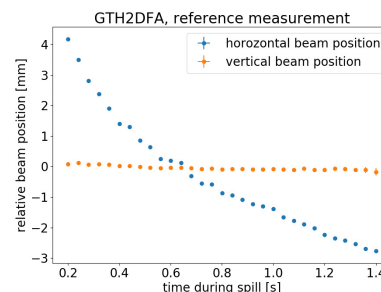


Figure 4: Movement of the beam during the spill.

stream screen while changing the strength of the magnet. Quadrupole strength variation rotates the phase space ellipse, the projections of beam ellipse are registered and its twiss parameters are calculated.

Horizontal Plane

The quadrupole scans were done in several locations, but here the one done using defocusing quadrupole GTH2QD12 and the screen GTH2DFA is presented. This combination is characterised by large distance between the quadrupole and the screen (18.7 meters) what simplifies the calculations allowing to use thin-lens approximation. The „video mode” of the system allows to split the spill into 40-ms slices, characterised by small $\Delta p/p$ what allows to neglect the dispersion.

Quadrupole-driven slow extraction process produces a beam with a very small horizontal emittance, in a form of „bar of charge”. In the first order approximation, the horizontal phase space has a uniform distribution in position (x) and a gaussian distribution in angle (x') at the electrostatic septum. However, the tracking simulation indicate that realistic distributions deviate from this approximation [6].

In order to be able to interpret the quadrupole scan measurement, in the following analysis we assume that the „bar of charge” has a uniform distribution with width a in x , Gaussian distribution in x' , and a is much smaller than $\sigma_{x'}$. A rotation of such ideal 2D distribution in phase space is illustrated in Fig. 5. For large range of rotation angles the obtained profile is Gaussian with $\sigma_x = a/\sqrt{12}$. Therefore, the results of the quadrupole scan can be interpreted in terms of double-Gaussian equivalent beam phase space distribution. During the quadrupole scan we have observed a good agreement of the measured beam distributions with Gaussian model (see Fig. 3), what does not prove but supports our approach.

Figure 6 shows the evolution of the horizontal beam width during the spill. The width grows, reaches maximum and slowly decays. This long decay corresponds to a period where the population of high-emittance particles decreases as they are being extracted (see Fig. 5.3 in [7] and [8]). In the maximum plateau, the particles of all emittances are extracted and this part of the spill is used for further analysis.

Figure 7 presents results of the quadrupole scan in horizontal plane, performed with the same silver beam as described in the previous section. The width of the beam

MC5: Beam Dynamics and EM Fields

D01 Beam Optics - Lattices, Correction Schemes, Transport

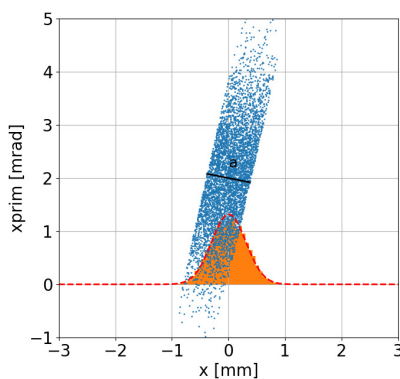


Figure 5: Conceptual illustration of phase space during the slow extraction and its projection.

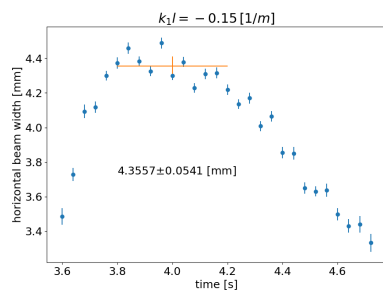


Figure 6: Horizontal beam width evolution during the spill. The red cross show the beam width taken to further analysis.

at the minimum of the parabola the beam is very small ($\approx 120\mu\text{m}$), reaching the limit of the system resolution, but exclusion of the two smallest beam size measurements does not change the fit results. The geometrical r.m.s. emittance is $0.018\mu\text{m}\mu\text{rad}$, and small values are expected in slow extracted beam (see Eq. 4.63 from [9]).

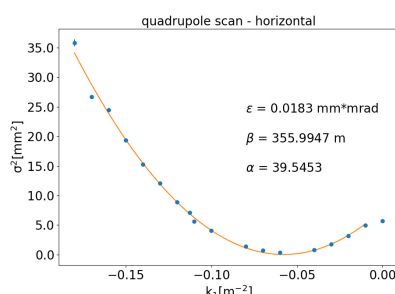


Figure 7: Results of the quad scan in horizontal plane $^{107}\text{Ag}^{45+}$ beam at 1580 MeV/u.

Vertical Plane

The signal in vertical plane obtained with analog camera was very noisy (see Fig.3), therefore the measurement was repeated on February 17th, 2019 using a new system with larger magnification and digital transmission. The beam was $^{12}\text{C}^{6+}$, with energy of 1450 MeV/u. Figure 8 shows the

MC5: Beam Dynamics and EM Fields

D01 Beam Optics - Lattices, Correction Schemes, Transport

profiles integrated over the spill duration and Fig. 9 presents results of the scan.

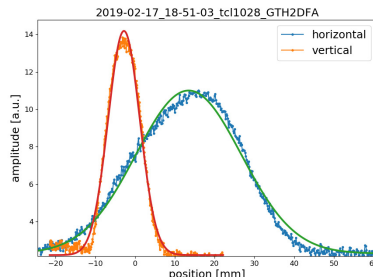


Figure 8: Beam profiles obtained with CUPID.

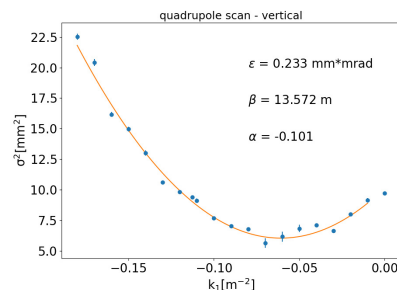


Figure 9: Results of the quad scan in vertical plane with $^{12}\text{C}^{6+}$ beam at 1450 MeV/u.

CONCLUSIONS

We presented some of the beam measurements performed on GSI High Energy Transfer lines, which is an important input for modelling and understanding the line. The study also presents the performance of various devices measuring beam profile.

ACKNOWLEDGEMENTS

Authors would like to thank to S. Sorge for discussions and M. Stein for implementing needed software features.

REFERENCES

- [1] G. Agakishiev *et al.*, "The High-Acceptance Dielectron Spectrometer HADES", *Eur. Phys. J. A* 41 (2009) 243.
- [2] M. Sapinski *et al.*, "Upgrade of GSI HADES Beam Line in Preparation for High Intensity Runs", in *Proc. IPAC'17*, Copenhagen, Denmark, May 2017, pp. 2214.
- [3] B. Walasek-Höhne *et al.*, "CUPID: New System for Scintillating Screen Based Diagnostics", in *Proc. IBIC'14*, Monterey, CA, USA, paper TUP014
- [4] <http://www.hauppauge.com/>
- [5] E. Jones, T. Oliphant, P. Peterson *et al.*, „SciPy: Open source scientific tools for Python”, <http://www.scipy.org/>
- [6] S. Sorge, priv. comm.
- [7] P.J. Bryant *et al.*, „Proton-Ion Medical Machine Study (PIMMS), Part II” CERN/PS 2000-007

[8] A. Wastl, et al., „Tomography of a Horizontal Phase Space Distribution of a Slow Extracted Proton Beam in the MedAustron High Energy Beam Transfer Line”, in *Proc. IPAC'15*, Richmond, USA, May 2015, pp. 3673.

[9] P.J. Bryant *et al.*, „Proton-Ion Medical Machine Study (PIMMS), Part I” CERN/PS 2000-007